

Article

Optimal Scheduling of Distributed Energy System for Home Energy Management System Based on Dynamic Coyote Search Algorithm

Chunbo Li ^{1,*}, Yuwei Dong ², Xuelong Fu ¹, Yalan Zhang ¹ and Juan Du ¹¹ Faculty of Electronic Information Engineering, Huaiyin Institute of Technology, Huai'an 223003, China² Department of Mechanical and Electronic Engineering, Jiangsu Vocational and Technical College of Finance and Economics, Huai'an 223003, China

* Correspondence: lcb@hyit.edu.cn

Abstract: Renewable and distributed power generation have been acknowledged as options for the safe, secure, sustainable, and cost-effective production, delivery, and consumption of energy in future low-carbon cities. This research introduces the Dynamic Coyote Search Algorithm (DCSA)-based optimal scheduling of distributed energy systems for home energy management systems. According to the heat storage properties of the building, a smart building energy model is established and introduced into the optimal scheduling of the distributed energy system in order to optimize the adjustment of the room temperature within the user's acceptable room temperature range. The DCSA algorithm used is to minimize the daily comprehensive operating cost, including environmental factors. According to the simulation results, the impact of smart energy storage on scheduling is analyzed, and the results show that the optimal scheduling of building smart energy storage participating in the system reduces the total cost by about 3.8%. In addition, the DCSA has a significantly faster convergence speed than the original coyote algorithm.



Citation: Li, C.; Dong, Y.; Fu, X.; Zhang, Y.; Du, J. Optimal Scheduling of Distributed Energy System for Home Energy Management System Based on Dynamic Coyote Search Algorithm. *Sustainability* **2022**, *14*, 14732. <https://doi.org/10.3390/su142214732>

Academic Editor: Akbar Maleki

Received: 2 October 2022

Accepted: 6 November 2022

Published: 8 November 2022

Publisher's Note: MDPI stays neutral with regard to jurisdictional claims in published maps and institutional affiliations.



Copyright: © 2022 by the authors. Licensee MDPI, Basel, Switzerland. This article is an open access article distributed under the terms and conditions of the Creative Commons Attribution (CC BY) license (<https://creativecommons.org/licenses/by/4.0/>).

Keywords: distributed energy system; optimal dispatch; Coyote Optimization Algorithm

1. Introduction

As environmental degradation and the energy problem continue to worsen, the energy system must be modified immediately. Distributed energy systems have the benefits of cost-effectiveness, environmental friendliness, and long-term viability, and have gained considerable interest, both domestically and internationally [1–3].

Rapid progress has been made in microgrid research as a result of the increasing use of renewable energy technology and distributed energy. Numerous studies have offered various approaches for addressing the unpredictability of renewable energy and load power. In ref. [4], the author considers the multi-interval-uncertainty constraints and analyzes the problem of microgrid robust scheduling analysis. In addition, the thermal insulation effect of the building wall and the heat storage property of the air improve the building's thermal inertia. When the characteristic quantity of the electrical equipment changes, there is a certain hysteresis phenomenon in the indoor temperature change [5]. Adjusting the temperature change curve within the user-acceptable temperature range can improve the flexibility of cooling (heating), which is of great significance for optimizing system operating costs. In ref. [6,7], the authors carried out modeling research on the smart energy storage of air-conditioning load, and the results showed the superiority and effectiveness of the smart energy storage strategy. In ref. [8], the author integrates smart energy storage into the combined heat and power energy system and proposes a strategy for stabilizing power fluctuations in the tie-line, and shows the effectiveness of this strategy through case studies. In ref. [9], the author established simultaneous smart energy storage models for electric vehicles and buildings, introduced them into the optimal scheduling of regional

integrated energy systems and established an economic optimal scheduling model with the goal of minimizing the daily operating cost of the system. In ref. [10], the author analyzed the optimal scheduling of smart energy storage for an electric refrigeration system and the combined cooling heating and power (CCHP) system. In ref. [11], the author considered the hybrid energy microgrids of four different buildings and conducted a dynamic economic optimal dispatch and comparative analysis based on building smart energy storage.

Recently, with the continuous development of intelligent optimization algorithms, choosing an appropriate optimization algorithm remains an important research topic in array synthesis. In ref. [12], the authors present a quantum evolutionary algorithm for optimizing the envelope layout of office buildings to the desired ENVLOAD (energy load of building envelope) value. The total cost is reduced by 35.3%, compared to the original design, and the construction cost per unit area of envelopes made from this paper is cheaper. In ref. [13], a combination of four optimization techniques is presented in order to optimally build a hybrid photovoltaic/diesel/battery nanogrid. The combined algorithms are executed in parallel, and the resulting solutions are compiled. A desert settlement in the Saudi Arabian city of Hafr Al-Batin serves as a test case. In ref. [14], the authors demonstrate that the Based on Hybrid Shuffled Frog-Leaping and Local Search Algorithm can lower system running expenses, and achieve the coordination and optimization of economy and robustness. In ref. [15], the author presents an optimized energy storage and distribution network model under the uncertainty of the power generation problem. Hybrid IGSA-DSO used an adoptive speed-inertia coefficient to ensure global and local searchability. Simulation shows interesting results for the proposed approach, which comparatively reduces the investment cost by 0.248%. The Coyote Optimization Algorithm (COA) [16] was proposed by Pierezan et al., in 2018, and shows strong optimization ability in the process of solving optimization problems. The COA includes a novel algorithm structure, fewer configurable parameters, and a simpler implementation compared to earlier algorithms. It offers a novel method for a balanced exploration and development, as well as improved convergence performance and optimization precision. However, when solving complex array antenna synthesis problems, the coyote optimization algorithm still has problems, for example, it has a slow convergence speed and falls easily into the local optimum.

This research presents a dynamic coyote search-based optimal scheduling for distributed energy systems for home energy management systems. On the basis of previous research, further research is now carried out to establish a smart energy storage model, according to the heat balance equation, in order to describe the process of smart energy storage participating in the optimal scheduling of the system. The objective function of the optimal scheduling process takes into account both the environmental cost and the comprehensive operation cost, and establishes a multi-objective optimal scheduling model based on economics. On the basis of the coyote algorithm, a suboptimal individual mutation approach and a global optimal intra-group guiding method are established in order to increase the local search capability and accelerate the convergence speed. Finally, the effect of smart energy storage on the dispatch outcomes is thoroughly examined in comparison to the dispatch situation without smart energy storage.

2. System Model Description

Figure 1 shows the structure of a typical distributed energy system, which primarily includes energy storage and conversion equipment such as batteries, absorption chillers, micro-turbines, and fans.

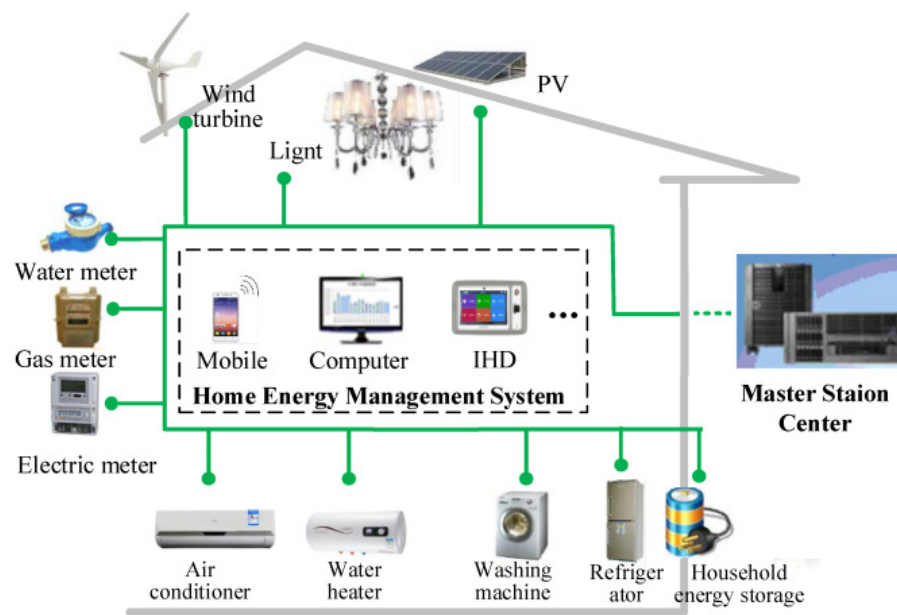


Figure 1. Typical distributed energy system for home energy management system.

The mathematical models for all of the equipment required in the home energy management system are as follows.

(1) Micro gas turbine model.

$$P_{MT} = P_{fuel} \eta_{MT} \quad (1)$$

where P_{MT} , and P_{fuel} are the output electric power and natural gas consumption power of the gas turbine, respectively, kW; η_{MT} are the power generation efficiency of the gas turbine.

(2) Absorption refrigerator model.

$$Q_{AR} = \eta_{HE} \lambda_{MT} P_{MT} COP_{AR} \quad (2)$$

where Q_{AR} is the output power of the absorption chiller, kW; η_{HE} are the efficiency of the heat exchange device; λ_{MT} is the thermoelectric ratio of the gas turbine; COP_{AR} is the cooling coefficient of the absorption refrigerant.

(3) Battery model.

Introducing the state of charge (SC) of the battery, the model is obtained as [17]

$$SC_{BT}^t = SC_{BT}^{t-1} (1 - \sigma_{BT}) + (\eta_{BT,ch} P_{BT,ch}^t - P_{BT,dis}^t / \eta_{BT,dis}) \Delta t / E_{BT} \quad (3)$$

where σ_{BT} is the self-discharge coefficient of the battery; $\eta_{BT,ch}$, $\eta_{BT,dis}$, are the charge and discharge efficiency of the battery, respectively; $P_{BT,ch}^t$, $P_{BT,dis}^t$ are the charge and discharge power of the battery, respectively; E_{BT} is the rated capacity of the battery, kW·h; t is the time.

(4) Building smart energy storage model.

The basic description equation is

$$\Delta Q = C \rho V (dT_{in} / dt) \quad (4)$$

where C is the specific heat capacity of air, J/(kg °C); ρ is the air density, kg/m³; V is the building volume capacity, m³; T_{in} is the indoor temperature, °C.

The factors that affect indoor heat primarily include temperature dissipation, caused by indoor and outdoor temperature difference; indoor heat source change; solar radiation; and output power of refrigeration equipment as

$$(K_{wall} S_{wall} + K_{win} S_{win}) (T_{out} - T_{in}) + G S_{win} S_c + Q_{in} - Q_{AR} = \rho C V \frac{dT_{in}}{dt} \quad (5)$$

where K_{wall} , K_{win} are the heat transfer coefficients of walls and windows, respectively, $W/(m^2 \cdot K)$; S_{wall} , S_{win} are the areas of walls and windows, respectively, m^2 ; T_{out} are the outdoor temperature, $^{\circ}C$; G is the light intensity on the outer surface of the window, kW/m^2 ; S_c is the shading coefficient, the value is 0.3; Q_{in} is the heating power of the indoor heat source, kW .

In order to better describe the smart energy storage, the smart energy storage charging and discharging power and the smart state of charge (SOVC) are introduced. The main parameters of the smart energy storage model are as follows.

$$\begin{cases} P = C\rho V(T_{in}^t - T_{in}^{t-1})/\Delta t \\ E = C\rho V(T_{in,max} - T_{in}^t) \\ E_B = C\rho V(T_{in,max} - T_{in,min}) \\ SOVC = \frac{E}{E_B} = \frac{T_{in,max} - T_{in}^t}{T_{in,max} - T_{in,min}} \end{cases} \quad (6)$$

where P is the charging and discharging power, kW ; E are E_B the capacity and rated capacity of the smart energy storage at a certain time, respectively, $kW \cdot h$; $T_{in,max}$, $T_{in,min}$ are the maximum and minimum acceptable indoor temperatures, $^{\circ}C$; the value of the air specific heat capacity $1000 J/(kg \cdot ^{\circ}C)$, the air density is $1.2 kg/m^3$.

3. Proposed Optimization Scheduling Model

3.1. Problem Formulation

The objective function aims for the lowest daily comprehensive cost. The daily comprehensive cost is composed of environmental cost and comprehensive operating cost (gas cost, electricity purchase and sales cost, and equipment maintenance cost). The specific expression of the objective function is:

$$F = F_{fuel} + F_{pu} + F_{om} + F_{en} \quad (7)$$

(1) Gas cost.

$$F_{fuel} = C_{fuel}P_{fuel} \quad (8)$$

where C_{fuel} is the cost of natural gas $\$/ (kW \cdot h)$, and P_{fuel} is measured, kW .

(2) Grid interaction costs.

$$F_{pu} = \sum_{t=1}^T C_{ph}^t P_{pg,buy}^t - \sum_{t=1}^T C_{se}^t P_{pg,sell}^t \quad (9)$$

where C_{ph} and C_{se} are the electricity purchase and electricity selling price; $P_{pg,sell}$ and $P_{pg,buy}$ are the electricity selling and electricity purchasing power, kW .

(3) Equipment maintenance costs.

$$F_{om} = \sum (P_{WT}^t C_{WT}^{om} + |P_{BT}^t| C_{BT}^{om} + P_{MT}^t C_{MT}^{om} + \lambda_{MT} P_{MT}^t C_{AC}^{om}) \quad (10)$$

where C_{WT}^{om} , C_{BT}^{om} , C_{MT}^{om} , C_{AC}^{om} are the maintenance costs of fans, batteries, micro-turbines, and absorption chillers, $\$/ (kW \cdot h)$; P_{WT}^t , P_{BT}^t , and P_{MT}^t are fans, batteries, and micro-turbines t time output power, kW .

(4) Environmental costs from the grid and gas turbines.

$$F_{en} = W_1 C_1 + W_2 C_2 \quad (11)$$

where W_1 and W_2 are the total purchased (generated) electricity of the power grid and the micro-gas turbine, $kW \cdot h$; C_1 and C_2 are the total treatment cost of the polluted gas brought by the power grid and the micro-gas turbine per $kW \cdot h$ of electricity, $\$/ (kW \cdot h)$.

The constraints

(1) Power balance constraints.

$$P_{ex,t} + P_{WT,t} + P_{MT,t} + P_{BT,t} = P_{el,t} \quad (12)$$

where $P_{el,t}$ is the electrical load demand of the building at time t , kW; $P_{ex,t}$ is the electrical load interacting with the grid at time t , kW.

(2) Cooling load balance constraints.

$$Q_{AR,t} = Q_{C,t} \quad (13)$$

where $Q_{C,t}$ is the cooling load of the building at time t , kW.

(3) Micro gas turbine output constraints.

$$P_{MT}^{\min} \leq P_{MT}^t \leq P_{MT}^{\max} \quad (14)$$

(4) Battery constraints.

$$\begin{cases} SC_{\min} \leq SC \leq SC_{\max} \\ P_{BT}^{\min} \leq P_{BT}^t \leq P_{BT}^{\max} \end{cases} \quad (15)$$

(5) Building thermal balance constraints.

$$\begin{aligned} \Delta t [K_{\text{wall}} S_{\text{wall}} (T_{\text{tout}} - T_{\text{tin}}) + K_{\text{win}} S_{\text{win}} (T_{\text{tout}} - T_{\text{tin}}) + G_t S_{\text{win}} S_c + Q_{\text{tin}} - Q_{\text{tAR}}] \\ = \rho C V (T_{t+1\text{in}} - T_{\text{tin}}) \end{aligned} \quad (16)$$

(6) Indoor temperature constraints.

$$T_{\text{in},\min} \leq T_{\text{in}} \leq T_{\text{in},\max} \quad (17)$$

3.2. Dynamic Coyote Search Algorithm (DCSA)

In the traditional coyote algorithm, the growth of the coyote is affected by the optimal alpha δ_1 and the cultural trend $cult_j$ in the group δ_2 . However, due to the initial random grouping, the quality of each group of alpha and the group's cultural orientation $cult_j$ cannot be guaranteed, and it is easy to have insufficient guiding ability of the optimal individuals in the group, falling into local optimum and a slow convergence speed. Moreover, the sub-optimal individual mutation strategy will inevitably increase the overall calculation amount of the algorithm and reduce the convergence speed, while improving the diversity of the population. In order to solve this problem, on the basis that the growth of each coyote is affected by δ_1 and δ_2 in the traditional coyote algorithm, a new growth method is constructed, and the intra-group guidance δ_3 of the global optimal Galpha is proposed. To guide the algorithm to approaching the global optimal solution faster, the local optimal solution must be exited, and the convergence speed must be increased. The updated Coyote algorithm is:

$$cult_j = \begin{cases} x_{(N_c+1)2,j} & N_c \text{ Odd No.} \\ (x_{N_c/2,j} + x_{N_c/2+1,j})/2 & N_c \text{ Even No.} \end{cases} \quad (18)$$

$$\delta_1 = \alpha - soc_{cr1}, \delta_2 = \alpha - soc_{cr2}, \delta_3 = \alpha - soc_{cr3} \quad (19)$$

$$soc_c^i = soc_c^0 + (\text{gen}/\text{Mgen})(r_1 \cdot \delta_1 + r_2 \cdot \delta_2) + (1 - \text{gen}/\text{Mgen})(r_3 \cdot \delta_3) \quad (20)$$

where $cult_j$ is the cultural trend within the group (x is the social status distribution of coyotes sorted in ascending order), obtained by calculating the median of all coyotes in the group, and N_c is the number of coyotes in the group. $cr1$, $cr2$, $cr3$ are the coyotes randomly selected in the group; Galpha is the global optimal; soc_c^0 , soc_c^i are the initial and updated social status of the coyote; gen is the current number of iterations; Mgen is the maximum number of iterations; r_1 , r_2 and r_3 represent the random weights of δ_1 , δ_2 and δ_3 , respectively; and δ_1 , δ_2 and δ_3 are random numbers uniformly distributed in the [0,1] interval.

The primary objective of the DCSA is to assign the ideal position update technique to each particle to allow the optimal solutions to the optimization issue to be located concurrently and more efficiently. The Galpha can be altered on a small scale by introducing

a Gaussian disturbance, with the assumption that it will travel in the direction of its closest peak, and the following status update is provided:

$$soc_{i,Nc}^{t+1} = \text{Galpha}_{i,Nc}(t) + \text{Gaussian}(0, \sigma) \quad (21)$$

where $\text{Gaussian}(0, \sigma)$ is the Gaussian distribution with mean zero and standard deviation σ .

The above cooperation can effectively avoid the waste of computing resources on memes with a poor evolutionary quality, and make full use of the evolutionary advantages of coyotes, thereby helping DCSA to fall into local optimal solutions and improving search efficiency.

The main steps of DCSA are described as follows:

- Step 1. Randomly generate an initial population soc_c^i , let r_1, r_2 and $r_3 = 0$
- Step 2. Divide the population into meme groups
- Step 3. Perform coyotes with dynamic search
- Step 4. Population reconstruction
- Step 5. Run the self-learning process
- Step 6. If the termination condition is satisfied, output the external file; otherwise go to step 2.

4. Results and Discussion

Two scheduling modes are introduced: mode 1 considers building smart energy storage and mode 2 does not consider building smart energy storage. When smart energy storage is not considered, the indoor temperature is 24°C during the working phase (8:00–19:45) and remains unchanged. The indoor temperature can vary between $(24 \pm 2)^\circ\text{C}$ when smart energy storage is taken into account. The building structure is 40 m long, 20 m wide, and each floor is 3 m high, with a total of 10 floors. As shown in Figure 2, the battery capacity is 40 kW·h, the battery self-discharge coefficient is 0.01, the charging and discharging efficiency is 0.95, the lower limit is in range of the charging power and discharge power is 100 kW and 30 kW, respectively. Figure 3 shows the impact of the light intensity as it reflects the light onto the outer surface of the window. Tables 1–3 show the building-related information, the time-of-use price used in the optimal scheduling process, and the values of the other main parameters.

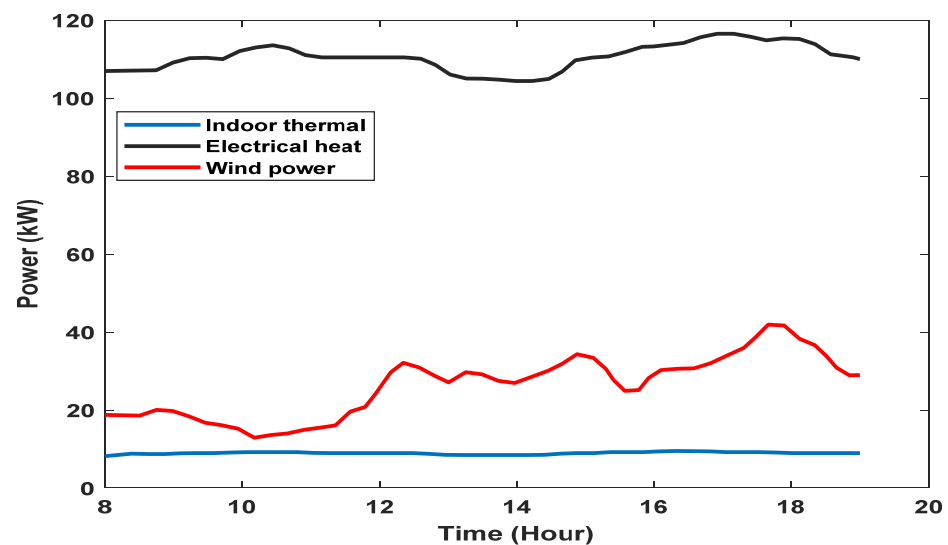


Figure 2. Electric load, wind power generation and indoor heat source.

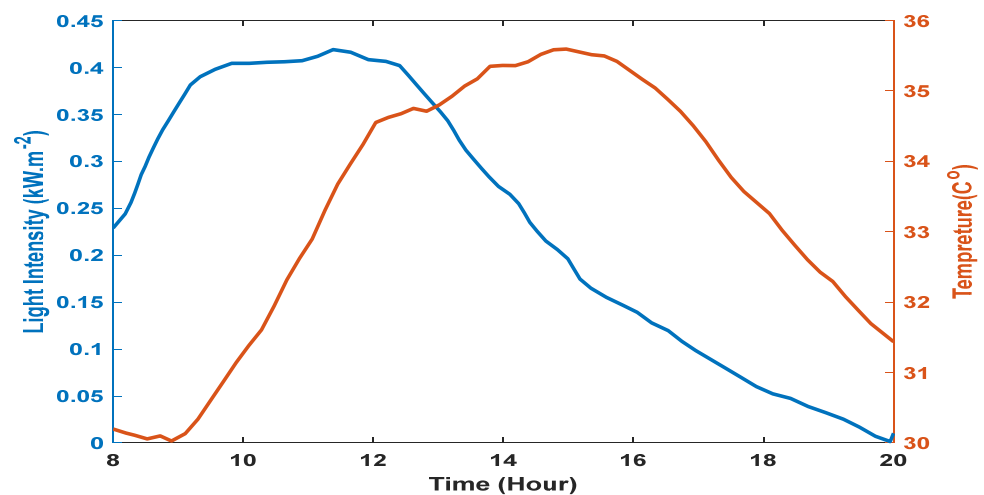


Figure 3. Outdoor temperature and light intensity.

Table 1. Building parameter.

Kwall	Swall	Kwin	Swin
$0.908 \text{ W}(\text{m}^2 \cdot \text{K})^{-1}$	3550 m^2	$2.750 \text{ W}(\text{m}^2 \cdot \text{K})^{-1}$	650 m^2

Table 2. Time-of-use electricity price.

Period	Electricity Purchase (\$)	Electricity (\$)	Time
Peak time	1.34	1.24	11:00—13:45, 18:00—19:45
Valley time	0.31	0.21	23:00—8:45
Normal	0.81	0.71	others

Table 3. Main parameter information table.

Parameter	Value
η_{MT}	0.3
λ_{MT}	1.5
η_{HE}	0.8
COP_{AR}	1.2
SOC_{min}/SOC_{max}	0.1/0.95
C_{WT}^{om}	0.11 \$/(kW·h)
C_{BT}^{om}	0.025 \$/(kW·h)
C_{MT}^{om}	0.03 \$/(kW·h)
C_{AC}^{om}	0.02 \$/(kW·h)

The system optimization scheduling process in the two cases is shown in Figures 4 and 5. Figure 4a,b compares the two dispatching scenarios. In the gas-fired power generation without smart energy storage, the most significant variation is in the external temperature and light intensity, which occurs when the system is operating in the mode of constant heat and electricity. In the low electricity price period, in order to reduce the gas cost when the smart energy storage participates in the scheduling, the gas turbine output is relatively small. During the high electricity price period in the afternoon, both systems will sell electricity to the grid to obtain benefits. However, after the smart energy storage participates in the scheduling, the gas turbine can be further increased. This is because the strong constraints on indoor temperature will be lifted when the smart energy storage participates in scheduling.

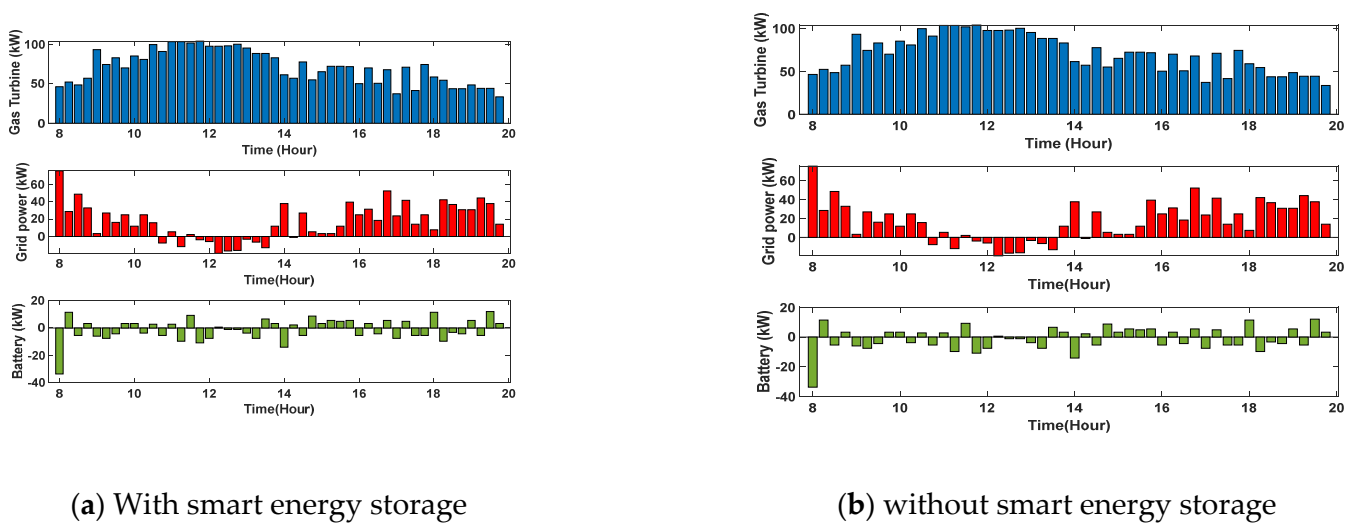


Figure 4. System optimization scheduling considering smart energy storage.

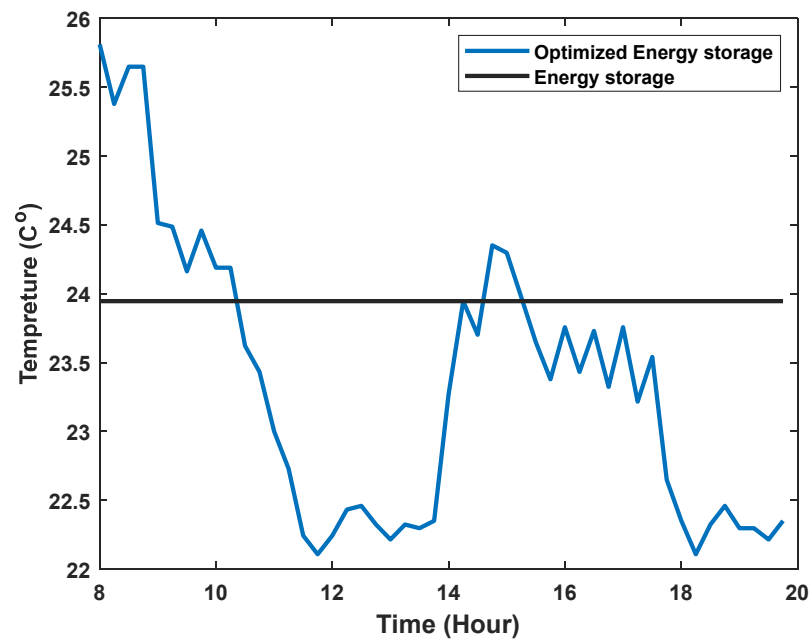


Figure 5. Room temperature curve.

Figure 5 shows that the room temperature fluctuates significantly after the participation of smart energy storage, and the building cooling load curve is optimized. In the period of high electricity price, which occurs at night due to the decrease of light intensity, the system's cooling load demand is greatly reduced, resulting in insufficient power generation of gas turbines. Subsequently, the insufficient power needs to be purchased from the grid. The cost of purchasing electricity decreased during this period.

The smart energy storage scheduling process is shown in Figure 6. It can be seen that the state of charge of the building smart energy storage maintains a relatively low level during the low electricity price period, the state of charge maintains a high level which indicating that the charging and discharging process can better follow the change of electricity price to achieve the purpose of reducing the overall cost of the system.

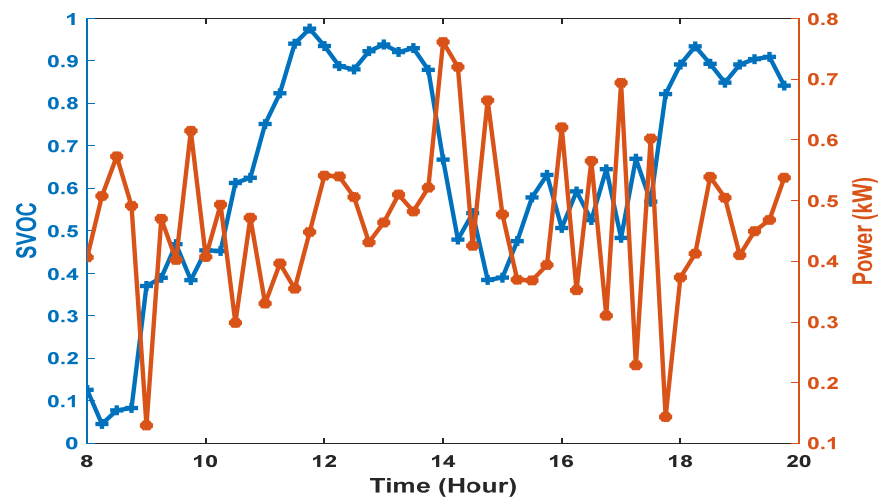


Figure 6. Output of smart energy storage.

Figure 7 shows the electricity purchase, sale, and cooling of the system. It can be seen that in the low electricity price period, due to the lower electricity purchase cost, there is no significant difference between the two scheduling situations. In mode 2, the rate of drop is approximately 13.93%, and the power purchase rate decreases by approximately 18.38% for the full period of high electricity prices. The electricity sales peak at midday, when prices are the highest. The electricity was 34.618 kW, an increase of approximately 136%. In addition, the total cooling load demand of the building is approximately 452.68 kW, without taking into consideration the building smart energy storage, and approximately 478.524 kW when considering it; the mode 1 increase is approximately 5.32%. From the data results, it can be seen that the building cooling load demand increases slightly after the participation of smart energy storage, but it brings great advantages to the purchase and sale of electricity in the system. Table 4 details the costs of the two dispatching modes. It can be seen that in the mode 1 dispatching scenario, the environmental cost is reduced by approximately 6.87% compared to mode 2, and the total cost of the entire dispatching process is reduced by approximately 3.74%, indicating that the participation of smart energy storage in dispatching can reduce system operation costs and has a positive impact on the control of environmental pollution.

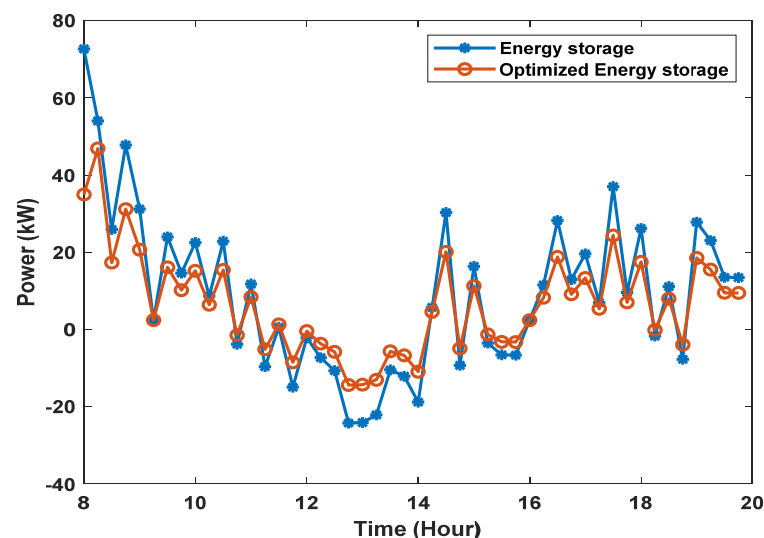
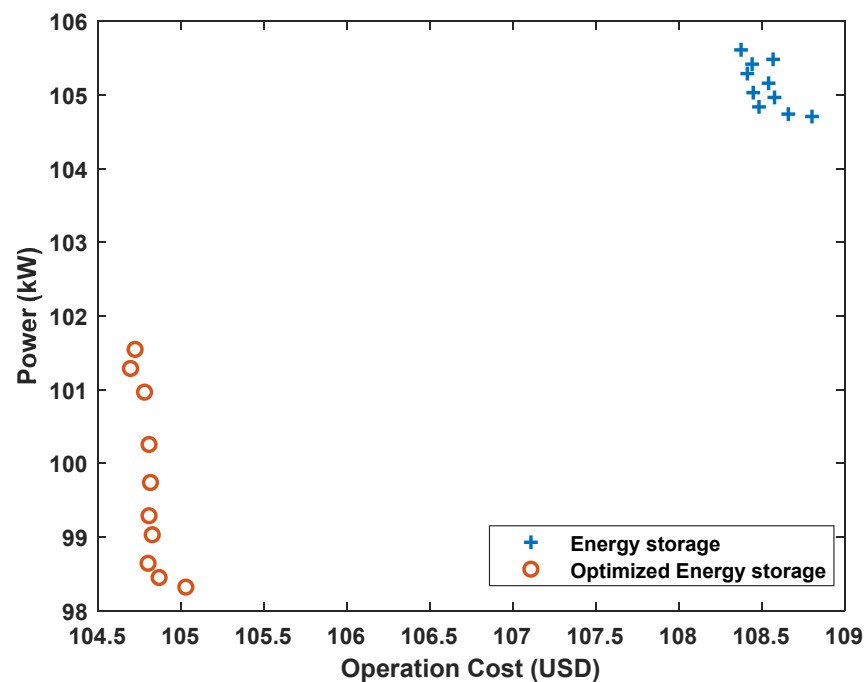


Figure 7. Purchase and sale of electricity.

Table 4. Cost Statistics.

Cost	Mode 1	Mode 2
Gas cost (USD)	63.43	61.02
Electricity cost (USD)	26.93	34.14
Electricity sales revenue (USD)	3.42	1.562
Operation and maintenance cost (USD)	11.73	12.37
Environmental cost (USD)	12.26	13.36
total cost (USD)	117.76	122.45

The DCSA algorithm parameters, following the population size of the algorithm, is set to 10; the number of iterations is 100; the learning factor $r_1 = r_2 = r_3 = 0.15$; and the initial inertia weight is 0.2548. Figure 8 shows the DCSA of the algorithm solution results in the two scheduling situations. It can be seen from the DCSA that the single pursuit of the minimum operating cost will increase the environmental cost, therefore, it is more practical to consider environmental factors in the actual process. At the same time, the multi-objective optimization process provides a number of different solutions for decision makers. The local environmental policy selects the most reasonable dispatch plan.

**Figure 8.** Optimized Energy storage using DCSA.

The final comparison of the processing times and operating costs for the two modes of the different algorithms is shown in Table 5. When the DCSA method is taken into account for the modes, mode 1's energy purchase price uncertainty is decreased by 4.013 USD (3.8%) compared to mode 2's. Additionally, for mode 1, the DCSA is reduced by 2.59 USD (2.45%), 3.7 USD (3.5%), and 3.7 USD (3.5%), respectively, in opposition to the COA and PSO. Therefore, it is evident that improving the mode's robustness requires forgoing some economic advantages after taking into account local and global optimal point issues of both algorithms. In addition, the time for the execution of the DCSA algorithm is reduced by 2.09 s (1.84%), and 2.73 s (2.4%), compared to the COA and PSO, respectively. Despite the fact that the DCSA algorithm significantly raises profit costs, the system is flexible enough to be altered in accordance with the current market electricity price and operational costs.

Table 5. Final comparison of operation mode with other optimization Algorithms.

Method	Energy Purchase Price (\$)		Time (s)
	Mode 1	Mode 2	
DCSA	105.62	109.63	113.64
COA	108.21	116.26	115.73
PSO	109.32	117.82	116.37

5. Conclusions

In this paper, a model for intelligent energy storage in buildings is developed and included in the optimal scheduling of distributed energy systems and the dynamic coyote search algorithm (DCSA). Through scheduling analysis, the usefulness of the smart energy storage plan participation is proven. The conclusions are as follows:

(1) The multi-objective optimization process shows that the single pursuit of the reduction of comprehensive operating costs will lead to an increase in environmental costs. Therefore, practically to take environmental factors in the optimal scheduling will have a positive effect on emissions and environmental protection.

(2) According to the purchase and sale of electricity, and the dispatching of gas turbines, building smart energy storage can improve the flexibility of the system's gas turbines and reduce the system's dependence on the power grid.

(3) In the process of participating in system optimization and scheduling, building smart energy storage can optimize the cooling load curve of the building, according to the electricity price, to reduce system operating costs, thereby improving the system economy.

(4) Based on Table 5, the proposed DCSA shows a better result, compared to both COA and PSO, as the selection mechanism improves the selection of the neighborhood size and distinguishes the particles in the neighborhood, between directly neighborhood-reachable and neighborhood-reachable, simultaneously, and thus balances the algorithm's exploration and exploitation.

Author Contributions: Formal analysis, Y.D. and Y.Z.; Investigation, X.F.; Methodology, J.D.; Writing—original draft, C.L. All authors have read and agreed to the published version of the manuscript.

Funding: This research received no external funding.

Institutional Review Board Statement: Not applicable.

Informed Consent Statement: Not applicable.

Data Availability Statement: Data is confidential.

Conflicts of Interest: The authors declare no conflict of interest.

References

- Hu, J.; Li, P. Energy-sharing method of smart buildings with distributed photovoltaic systems in area. *Energy Rep.* **2022**, *8*, 622–627. [CrossRef]
- Yan, Y.; Zhang, H.; Meng, J.; Long, Y.; Zhou, X.; Li, Z.; Wang, Y.; Liang, Y. Carbon foot-print in building distributed energy system: An optimization-based feasibility analysis for potential emission reduction. *J. Clean. Prod.* **2019**, *239*, 117990. [CrossRef]
- Liu, Z.; Fan, G.; Sun, D.; Wu, D.; Guo, J.; Zhang, S.; Yang, X.; Lin, X.; Ai, L. A novel distributed energy system combining hybrid energy storage and a multi-objective optimization method for nearly ze-ro-energy communities and buildings. *Energy* **2022**, *239*, 122577. [CrossRef]
- Levorato, M.; Figueiredo, R.; Frota, Y. Robust microgrid energy trading and scheduling under budgeted uncertainty. *Expert Syst. Appl.* **2022**, *203*, 117471. [CrossRef]
- Delfino, F.; Ferro, G.; Minciardi, R.; Robba, M.; Rossi, M.; Rossi, M. Identification and optimal control of an electrical storage system for microgrids with renewables. *Sustain. Energy Grids Netw.* **2019**, *17*, 100183. [CrossRef]
- Mishra, R.; Chaulya, S.; Prasad, G.; Mandal, S.; Banerjee, G. Design of a low cost, smart and stand-alone PV cold storage system using a domestic split air conditioner. *J. Stored Prod. Res.* **2020**, *89*, 101720. [CrossRef]
- Qi, N.; Cheng, L.; Xu, H.; Wu, K.; Li, X.; Wang, Y.; Liu, R. Smart meter data-driven evaluation of operational demand response potential of residential air conditioning loads. *Appl. Energy* **2020**, *279*, 115708. [CrossRef]

8. Shabgard, H.; Song, L.; Zhu, W. Heat transfer and exergy analysis of a novel solar-powered integrated heating, cooling, and hot water system with latent heat thermal energy storage. *Energy Convers. Manag.* **2018**, *175*, 121–131. [[CrossRef](#)]
9. Calise, F.; Cappiello, F.L.; d'Accadia, M.D.; Vicidomini, M. A novel smart energy net-work paradigm integrating combined heat and power, photovoltaic and electric vehicles. *Energy Convers. Manag.* **2022**, *260*, 115599. [[CrossRef](#)]
10. Abdalla, A.N.; Nazir, M.S.; Tiezhu, Z.; Bajaj, M.; Sanjeevikumar, P.; Yao, L. Optimized Economic Operation of Microgrid: Combined Cooling and Heating Power and Hybrid Energy Storage Systems. *J. Energy Resour. Technol.* **2021**, *143*, 070906. [[CrossRef](#)]
11. Nazir, M.S.; Abdalla, A.N.; Wang, Y.; Chu, Z.; Jie, J.; Tian, P.; Jiang, M.; Khan, I.; Sanjeevikumar, P.; Tang, Y. Optimization configuration of energy storage capacity based on the microgrid reliable output power. *J. Energy Storage* **2020**, *32*, 101866. [[CrossRef](#)]
12. Wang, Y.; Wei, C. Design optimization of office building envelope based on quantum genetic algorithm for energy conservation. *J. Build. Eng.* **2020**, *35*, 102048. [[CrossRef](#)]
13. Bouchekara, H.R.E.H.; Shahriar, M.S.; Irshad, U.B.; Aban, Y.A.S.; Mahmud, M.A.P.; Javaid, M.S.; Ramli, M.A.M.; Farjana, S.H. Optimal sizing of hybrid photovoltaic/diesel/battery nanogrid using a parallel multiobjective PSO-based approach: Application to desert camping in Hafr Al-Batin city in Saudi Arabia. *Energy Rep.* **2021**, *7*, 4360–4375. [[CrossRef](#)]
14. Abdalla, N.A.; Ju, Y.; Nazir, M.S.; Tao, H. A Robust Economic Framework for Integrated Energy Systems Based on Hybrid Shuffled Frog-Leaping and Local Search Algorithm. *Sustainability* **2022**, *14*, 10660. [[CrossRef](#)]
15. Nazir, M.S.; Abdalla, A.N.; Zhao, H.; Chu, Z.; Nazir, H.M.J.; Bhutta, M.S.; Javed, M.S.; Sanjeevikumar, P. Optimized economic operation of energy storage integration using improved gravitational search algorithm and dual stage optimization. *J. Energy Storage* **2022**, *50*, 104591. [[CrossRef](#)]
16. Pierezan, J.; Coelho, L.D.S. Coyote Optimization Algorithm: A New Metaheuristic for Global Optimization Problems. In *2018 IEEE Congress on Evolutionary Computation (CEC)*; IEEE: Piscataway Township, NJ, USA, 2018; pp. 1–8.
17. Barbosa, V.; Nogueira, T.; Carati, E.; Felgueiras, C. Supercapacitor in battery charges of photovoltaic panel: Analysis of the technical feasibility. *Energy Procedia* **2018**, *153*, 80–85. [[CrossRef](#)]